

$A(L)$ of the coexistence curve, $\Delta n = A(L)\{[T_c(L) - T]/T_c(\infty)\}^{\beta_2}$, should also scale^{1,2} with L : $A(L) \propto L^{(\beta_2 - \beta_3)\theta}$, where the subscript on β is the "dimensionality." Our data as plotted in Fig. 3 suggest that the amplitude $A(L)$ varies as L^z with z in the range 0.6 to 0.8. With β_2 taken to be our experimental value of 0.5 and $\beta_3 = 0.326$,¹⁶ then $\theta = 4 \pm 0.5$.

In conclusion, our experimental results on the critical-temperature shift suggest a logarithmic dependence on film thickness for thick films ($1 \mu\text{m} \leq L \leq 60 \mu\text{m}$). A "mean-field" value of $\beta = 0.5$ was determined from the coexistence curve data taken close to $T_c(L)$ for film thicknesses $\leq 6 \mu\text{m}$. These results are consistent with each other and suggest that long-range interactions are present, rather than the lattice-gas behavior expected. It is not clear to what extent the walls constraining the fluid mixture affect its critical behavior.

Further experiments are in progress.

*Supported in part by the U. S. Energy Research and Development Administration under Contract No. E(11-1)-2203.

†Present address: Physics Department, College of Wooster, Wooster, Ohio 44691.

¹M. E. Fisher, in *Critical Phenomena, Proceedings of the International School of Physics, "Enrico Fermi"*, Course No. LI, edited by M. S. Green (Academic, New

York, 1971), p. 1, and Rev. Mod. Phys. **46**, 597 (1974).

²D. J. Bergman, Y. Imry, G. Deutscher, and S. Alexander, J. Vac. Sci. Technol. **10**, 674 (1973).

³D. P. Landau, Phys. Rev. B **13**, 2997 (1976), and references contained therein.

⁴D. F. Brewer, J. Low Temp. Phys. **3**, 205 (1970).

⁵E. Guyon, J. Vac. Sci. Technol. **10**, 681 (1973).

⁶R. J. Birgeneau, H. J. Guggenheim, and G. Shirane, Phys. Rev. B **1**, 2211 (1970).

⁷H. Lutz, J. D. Gunton, H. K. Schurmann, J. E. Crow, and T. Mihalisin, Solid State Commun. **14**, 1075 (1974).

⁸G. A. Hawkins and G. B. Benedek, Phys. Rev. Lett. **32**, 524 (1974); M. W. Kim and D. S. Cannell, Phys. Rev. A **13**, 411 (1976).

⁹Coating is Perkin Elmer, HHFD, 90.0% reflectance at 6328 Å.

¹⁰K. B. Lyons, R. C. Mockler, and W. J. O'Sullivan, Phys. Rev. A **10**, 393 (1974).

¹¹B. A. Scheibner, C. Wells, D. T. Jacobs, R. C. Mockler, and W. J. O'Sullivan, to be published.

¹²C. Warren and W. W. Webb, J. Chem. Phys. **50**, 3694 (1969).

¹³D. T. Jacobs, D. J. Anthony, R. C. Mockler, and W. J. O'Sullivan, to be published.

¹⁴W. I. Goldberg and P. N. Pusey, J. Phys. (Paris), Colloq. **33**, C1-105 (1972).

¹⁵S. Miyazima, J. Phys. Soc. Jpn. **35**, 68 (1973).

¹⁶C. L. Hartley, D. T. Jacobs, R. C. Mockler, and W. J. O'Sullivan, Phys. Rev. Lett. **33**, 1129 (1974).

¹⁷It is shown in Ref. 13 that the difference in refractive index is proportional to the difference in volume fraction for these fluids.

¹⁸C. L. Hartley, Ph.D. thesis, University of Colorado, 1974 (unpublished).

Longitudinal Optical Vibrations in Glasses: GeO_2 and SiO_2

F. L. Galeener and G. Lucovsky

Xerox Palo Alto Research Center, Palo Alto, California 94304

(Received 29 July 1976)

We show that longitudinal optical (LO) vibrational modes account for several previously unexplained peaks in the Raman spectra of vitreous GeO_2 and SiO_2 . Identification of LO modes in these and other glasses reduces the complexity of the spectra that must be explained by simple structural models. It also follows that long-range (Coulomb) forces should be included in complete theories of the vibrational properties of many glasses.

The Raman spectra of vitreous germania ($v\text{-GeO}_2$) and vitreous silica ($v\text{-SiO}_2$) have long been puzzling because each contains peaks which have not been explained by vibrational calculations based on the favored structural model. The presently favored model, proposed in 1932 by Zachariasen,¹ asserts that $v\text{-SiO}_2$ is primarily a continuous network of nearly perfect SiO_4 tetrahedra connected to each other in such a way that each corner oxygen atom is shared by a different neighboring tetrahedral unit, thus preserving the chem-

ical formula. The disorder that is characteristic of glasses is accounted for by allowing large variations in the orientation of neighboring tetrahedra. This structure is also thought to be appropriate for $v\text{-GeO}_2$ and for several other glasses, such as $v\text{-BeF}_2$, $v\text{-ZnCl}_2$, and $v\text{-GeS}_2$.

The Zachariasen model is especially attractive because it raises the possibility that many properties can be treated by focusing attention on a single representative tetrahedral unit, and by assuming simple statistical laws for the orientation

of the neighbors. Using this model, Mozzi and Warren² have accounted satisfactorily for all the features seen in the x-ray radial distribution function of v -SiO₂.

The situation has not proved so simple in the case of the vibrational properties of these glasses. Historically, it was found that the vibrational frequencies of an isolated tetrahedral unit are too few in number to explain all of the observed Raman features, and often do not coincide quantitatively with many of the observed features. Attempts were made to remedy this by choosing larger "molecular" units, in order to increase the number of predicted normal modes,³ and by resorting to quasicrystalline or microcrystalline models.⁴ These alternative approaches have not produced convincing improvements; we view them as tractable efforts to take into account the interactions of a representative tetrahedron with its nearest neighbors. This general approach has culminated in the much more comprehensive calculations of Bell and co-workers,⁵ which are based on large (~600 atom) clusters of almost perfect tetrahedral units interacting with each other via short-range (nearest-neighbor) bond forces. In this Letter, we will demonstrate that a complete explanation of the vibrational spectra requires incorporation of another type of interaction between the tetrahedra, viz., the *long-range* interaction provided by the Coulomb fields associated with certain excitations of the system.

We will first consider the case of germania. Figure 1 shows the polarized Raman spectra and

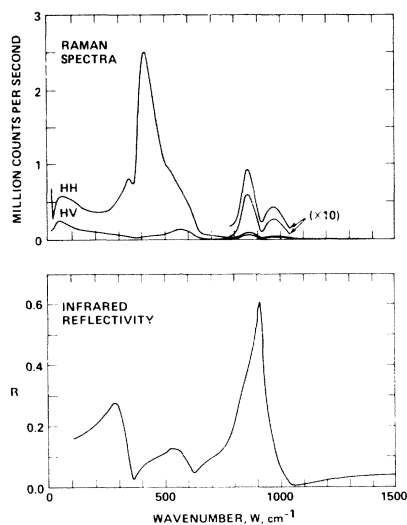


FIG. 1. The Raman spectra and infrared reflectivity of bulk vitreous germania at room temperature.

the infrared (IR) reflectivity which we obtained from a bulk sample of high-purity v -GeO₂ maintained at room temperature. This particular sample has very low OH content (<5 ppm) and shows no bubbles under microscopic examination; the total level of metallic impurities appears to be quite low (absence of color and luminescence) but is not precisely known. The Raman intensities were obtained in the 90° configuration using a Spex 1401 double monochromator, an RCA 31034A photomultiplier, an SSR-1110 photon counting system, and approximately 3.5 W of 5145-Å radiation from a CR-12 Ar⁺ ion laser. The IR spectrum was obtained with a Perkin-Elmer Model 180 spectrometer equipped with reflectance attachment. In both cases, resolution was better than 5 cm⁻¹.

Figure 2 compares the reduced Raman spectra⁶ with the density of vibrational states derived by Bell and Dean.⁷ The solid curve represents the density of states for the condition that the surface atoms of the cluster (all oxygen) are fixed in their equilibrium positions, while the dashed line is the result when the surface atoms are allowed to move freely. In the spirit of the theory of Shuker and Gammon,⁸ we interpret the density of states as composed of separate sub-bands, each of which shows up in the Raman spectra with a relative strength depending on the magnitude of an appropriate multiplicative coupling coefficient. From this point of view, the cluster calculation can be viewed as accounting for all of the clear features in the HH and HV spectra except for

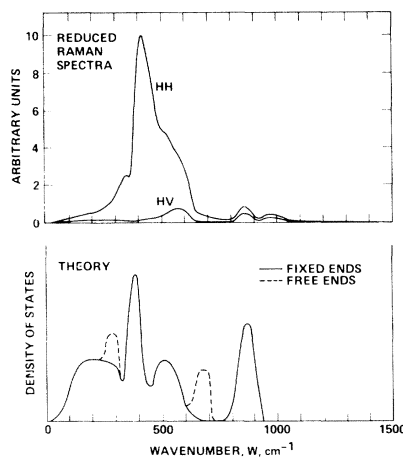


FIG. 2. Comparison of the room-temperature reduced Raman spectra of bulk v -GeO₂ with the theoretical density of vibrational states reported by Bell and Dean (Ref. 7).

two—the sharp peak at $\sim 347 \text{ cm}^{-1}$ and the very broad peak at $\sim 973 \text{ cm}^{-1}$. These two peaks (and similar ones seen in $v\text{-SiO}_2$) have been ascribed to defects, impurities, dangling oxygens, and other inadequacies of the continuous-network structural model. We shall show that they are *not* due to inadequacies of the structural model, but are due to the existence of long-range Coulomb or electromagnetic forces. These forces have not been considered in formal treatments of the vibrational properties of glasses, which proceed traditionally from the molecular or short-range interaction point of view.⁹

It is common in studies of polarizable media such as plasmas and polar crystals to discern two types of macroscopic modes: transverse and longitudinal.¹⁰ In an isotropic medium (such as a glass), transverse modes are those in which the average electric vector \bar{E} is perpendicular to the direction of periodicity of the wave; their resonant frequencies are determined by poles in $\epsilon_2 \equiv \text{Im}(\epsilon)$, where ϵ is the complex dielectric function of the medium. Longitudinal modes are a complementary set whose average electric field is completely parallel to the direction of periodicity. Longitudinal modes resonate at zeros of ϵ ; in the long wavelength limit assumed in the present work, they resonate at poles of the dielectric energy-loss function $\text{Im}(-1/\epsilon)$. Converse statements follow: Peaks in ϵ_2 reveal transverse modes, while peaks in $\text{Im}(-1/\epsilon)$ identify longitudinal modes.¹¹

To investigate the possibility of longitudinal response in our $v\text{-GeO}_2$ Raman data, we have therefore determined the poles in ϵ_2 and $\text{Im}(-1/\epsilon)$, and have compared their positions with those of the observed Raman peaks. Kramers-Kronig techniques were applied to the reflectivity data in Fig. 1 in order to extract IR values of $\epsilon = \epsilon_1 + i\epsilon_2$; and the latter were used to compute $\text{Im}(-1/\epsilon) = \epsilon_2/(\epsilon_1^2 + \epsilon_2^2)$. The validity of this procedure for predicting the position and shape of Raman-active LO modes from reflectivity data has been demonstrated by Barker in studies of crystalline GaP.¹²

Our results for $v\text{-GeO}_2$ are presented in Fig. 3. It is immediately evident that the mysterious features at 347 and 973 cm^{-1} in the Raman spectrum correspond very closely to distinct peaks at the same frequencies in the energy-loss function; even the linewidths are comparable. It is therefore reasonable to assume that the Raman spectrum reveals the existence of longitudinal optical excitations centered at 347 and 973 cm^{-1} , which are associated with transverse optical (TO) excita-

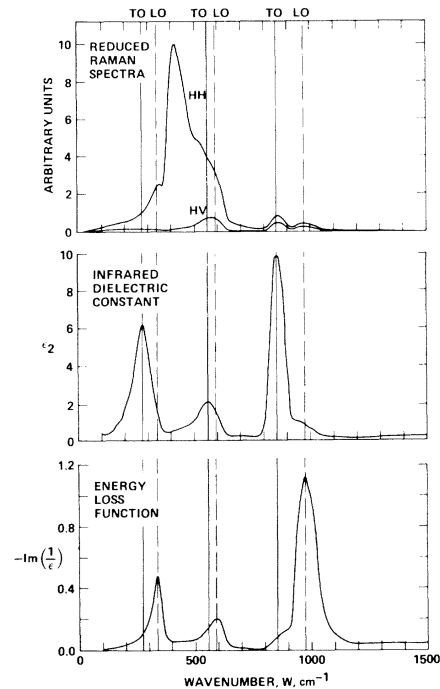


FIG. 3. Comparison of reduced Raman spectra of bulk $v\text{-GeO}_2$ with the experimentally determined transverse energy-loss function ϵ_2 and the longitudinal energy-loss function, $\text{Im}(-1/\epsilon)$. Note the identification of Raman lines at 347 and 973 cm^{-1} as longitudinal optical (LO) modes.

tions centered at ~ 278 and $\sim 857 \text{ cm}^{-1}$, respectively. It also appears that there is an LO excitation centered at $\sim 595 \text{ cm}^{-1}$, associated with a TO mode at $\sim 556 \text{ cm}^{-1}$, although these two lines do not appear as separate peaks in the Raman spectrum.¹³

We refer to the above modes as *optical* because they appear at sufficiently high frequencies to obviate the possibility of their being acoustic, using the usual nomenclature applied to crystals. Also, since there is as yet no microscopic theory of the vibrational motions involved, we presently restrict the meaning of transverse and longitudinal to that specified earlier, namely by the nature of the average electric field in a macroscopic polarization wave. It is unlikely that the microscopic *displacements* in a TO mode are transverse to the macroscopic periodicity; however, more precise specification of the connection should prove quite informative.

Similar results have been obtained in studies of fused silica, as illustrated in Fig. 4. The solid curves were obtained from Raman scattering and IR reflectivity measurements¹⁴ on a bulk sample of high-purity Suprasil W-1. This material is

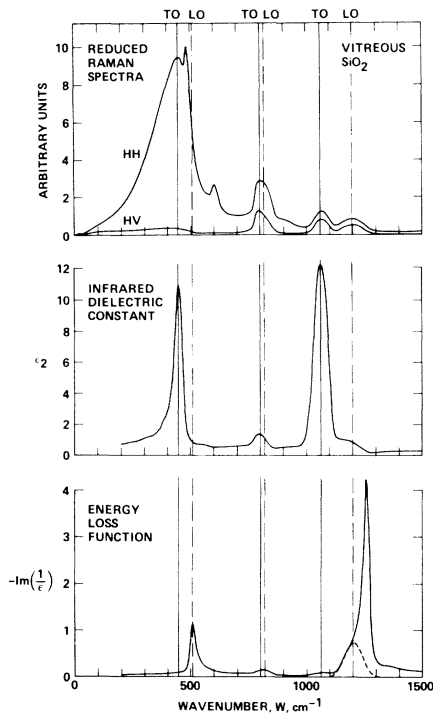


FIG. 4. Comparison of the reduced Raman spectra with ϵ_2 and $\text{Im}(-1/\epsilon)$, obtained from a bulk sample of $v\text{-SiO}_2$ at room temperature. With the help of other information mentioned in the text, we deduce that the Raman peaks seen at 495 and 1200 cm^{-1} are LO modes.

known to have low OH content (<5 ppm), low metallic impurity levels (total <1 ppm), and extremely low bubble content.¹⁵ Comparison of the observed HH Raman spectrum with the calculations of Bell and Dean⁷ reveals that the sharp line at 495 cm^{-1} and the broad peak at 1200 cm^{-1} are entirely unpredicted.

Although the correspondence with peaks in $\text{Im}(-1/\epsilon)$ is not as perfect as in the case of $v\text{-GeO}_2$,¹⁶ we feel confident that the Raman data in $v\text{-SiO}_2$ also reveals three TO-LO pairs, at approximately the following frequencies: 455 and 495 cm^{-1} ; 800 and 820 cm^{-1} ; 1065 and 1200 cm^{-1} . This confidence is based on analogy with the unequivocal $v\text{-GeO}_2$ data, and on several other observations. For example, the above TO-LO frequencies compare quite favorably with the major pairs reported in crystalline α -quartz by Scott and Porto¹⁷: 450 and 509 cm^{-1} ; 795 and 807 cm^{-1} ; 1072 and 1235 cm^{-1} . Also, our studies of the Raman spectra of numerous samples of $v\text{-SiO}_2$ indicate that the lines identified as LO are characteristic of the SiO_2 network rather than defects or impurities; the LO Raman lines do not change in

strength or position with large variations in water content,^{18,19} metallic impurity levels,²⁰ or microscopic bubble content.²⁰

This work raises a number of interesting questions. How many glasses have sufficient polarizability to exhibit TO-LO splittings? We have preliminary evidence for the existence of split-off LO modes in the Raman spectra of $v\text{-BeF}_2$ and $v\text{-B}_2\text{O}_3$, and expect their occurrence in numerous other glasses. Does a TO-LO pair in a glass represent two distinct peaks in the density of states, or is their separateness caused only by Raman matrix-element effects? The 1065- cm^{-1} and 1200- cm^{-1} peaks in $v\text{-SiO}_2$ appear as distinct but broadened features in the neutron scattering data of Leadbetter and Stringfellow²¹; it thus appears that this particular TO-LO pair is associated with separate peaks in the total density of states. Improved inelastic neutron scattering data on $v\text{-SiO}_2$ and similar data on $v\text{-GeO}_2$ will help resolve the questions for the other TO-LO pairs. The longitudinal nature of the LO modes may be verified independently by carrying out very-high-resolution electron energy-loss experiments. Incorporation of Coulomb forces into cluster calculations would be deeply satisfying and would enable the extraction of meaningful effective charges from the TO-LO splittings. It is evident that the effective charges must be large and that they may cause effects in addition to the ones that we have noted. Polaron effects are a likely example. Finally, the observation of TO-LO splittings in disordered solids suggests their possible appearance in the Raman spectra of highly polarizable *liquids*.

We are grateful to Professor D. Turnbull of Harvard University and to Dr. R. H. Stolen of Bell Laboratories, who kindly provided us with the high-quality samples of $v\text{-GeO}_2$ used in this study. We are also grateful to Mr. W. J. Mosby for skillful acquisition of the Raman spectra, and to Mrs. M. Rodoni for assistance in computer analysis of the results. We are further indebted to Professor R. M. Pick, Dr. R. M. Martin, and Dr. P. N. Sen for helpful discussions.

¹W. H. Zachariasen, J. Am. Chem. Soc. **54**, 3841 (1932).

²R. L. Mozzi and B. E. Warren, J. Appl. Crystallogr. **2**, 164 (1969).

³For an early review, see I. Simon in *Modern Aspects of the Vitreous State*, edited by J. D. Mackenzie (Butterworths, London, 1960), Vol. I, p. 120.

⁴For an interesting recent example, see J. B. Bates, J. Chem. Phys. **56**, 1910 (1972).

⁵R. J. Bell and P. Dean, *Discuss. Faraday Soc.* **50**, 55 (1970).

⁶J. E. Smith, Jr., M. H. Brodsky, B. L. Crowder, and M. I. Nathan, in *Proceedings of the Second International Conference on Light Scattering in Solids*, edited by M. Balkanski (Flammarion, Paris, 1971), p. 330.

⁷R. J. Bell and P. Dean, in *Amorphous Materials*, edited by R. W. Douglas (Wiley-Interscience, London, 1972), p. 443.

⁸R. Shuker and R. W. Gammon, *Phys. Rev. Lett.* **25**, 222 (1970).

⁹Infrared effective charges for ν -As₂S₃ and ν -As₂Se₃ have been estimated by G. Lucovsky, *Phys. Rev. B* **6**, 1480 (1972); however, the connection between LO modes and Raman features was not discussed.

¹⁰C. Kittel, *Introduction to Solid State Physics*, (Wiley, New York, 1971), 4th ed., p. 183.

¹¹In all our results on glasses, the observed poles in $\text{Im}(-1/\epsilon)$ occur at the same wave number values as the zeros in $\epsilon_1 \equiv \text{Re}(\epsilon)$, within instrumental resolution.

¹²A. S. Barker, Jr., *Phys. Rev.* **165**, 917 (1968).

¹³In the absence of a theory that includes Coulomb effects, we have no first-principles method for predicting the number of *observable* TO-LO splittings in a glass.

¹⁴See also F. L. Galeener and G. Lucovsky, in *Struc-*

ture and Excitations of Amorphous Solids (American Institute of Physics, New York, 1976), p. 223.

¹⁵Samples and specifications obtained from Amersil, Inc., 685 Ramsey Ave., Hillside, N. J. 07205.

¹⁶We do not yet understand the discrepancies, especially the sharpness and position of the 1260-cm⁻¹ peak in $\text{Im}(-1/\epsilon)$. Some explanations which we still think possible are (1) unidentified problems with sample reflectivity, (2) an inappropriateness for ν -SiO₂ of the exact combination $\epsilon_2/(\epsilon_1^2 + \epsilon_2^2)$, and (3) a true matrix-element effect, not present in ν -GeO₂.

¹⁷J. F. Scott and S. P. S. Porto, *Phys. Rev.* **161**, 903 (1967).

¹⁸For precise quantitative studies of the Raman spectra of bulk samples of ν -SiO₂ containing OH in concentration of < 5 ppm, ~ 180 ppm, and ~ 1200 ppm, see F. L. Galeener and R. H. Geils, to be published.

¹⁹Also see R. H. Stolen and G. E. Walrafen, *J. Chem. Phys.* **64**, 2638 (1976), in which they report a small reduction in strength of the 495-cm⁻¹ Raman line for samples with OH concentration ~ 1350 ppm. We do not see this reduction in our samples.

²⁰F. L. Galeener, to be published.

²¹A. J. Leadbetter and M. W. Stringfellow, in *Neutron Inelastic Scattering* (International Atomic Energy Agency, Vienna, 1974), p. 501

“Critical” Slowing Down at the Roughening Transition

Robert H. Swendsen*

Institut für Festkörperforschung der Kernforschungsanlage Jülich, D-5170 Jülich, Germany

(Received 26 July 1976)

The existence of “critical” slowing down at the roughening transition in Monte Carlo simulations of both the kinetic solid-on-solid model and discrete Gaussian model is reported. Comparison with critical behavior at the more usual second-order phase transitions shows both similarities and differences that shed light on the nature of the roughening transition. The roughening temperature is found to be $k_B T_K = (1.15 \pm 0.05)\epsilon$ for the solid-on-solid model.

The roughening transition in an interface between two phases in a three-dimensional Ising model has been of interest since Burton and Cabrera¹ first suggested in 1949 that the interface width should diverge at a temperature, T_R , far below the bulk critical temperature. Since the lattice-gas interpretation of this model is widely used in the theory of crystal growth and since roughening should significantly affect both growth rates and crystal perfection,² a good understanding of the transition is essential.

In this Letter, I report the existence of “critical” slowing down at the roughening transition in a Monte Carlo simulation of the kinetic solid-on-solid (SOS) model of a crystal surface³⁻⁶ [this is just the kinetic Ising model in the limit of infinitely strong interactions perpendicular to the interface: $T_c^{\text{SOS}} = \infty$]. By comparing this phenom-

enon with critical behavior at the more usual second-order phase transitions, I find both similarities and differences that provide insight into the nature of the roughening transition. In addition to accurate values for the static and dynamic properties of the system, our results include the best current estimate of the roughening temperature, $k_B T_R = (1.15 \pm 0.05)\epsilon$.⁷ This value is much closer to the transition temperature for the corresponding two-dimensional Ising model ($k_B T_c^{2D} = 1.13459\epsilon$) than previous values⁸ to be discussed below.

In the SOS model, the height of the surface at each site, h_{ij} , takes on integral values and is described by the Hamiltonian

$$\mathcal{H} = \epsilon \sum_i \sum_j (|h_{i,j} - h_{i+1,j}| + |h_{i,j} - h_{i,j+1}|). \quad (1)$$

The kinetics are introduced in the usual way as